0021-972X/05/$15.00/0
*Printed in U.S.A.*

The Journal of Clinical Endocrinology & Metabolism 90(9):5134–5140

doi: 10.1210/jc.2004-1778

# Detection of Adrenocorticotropin-Secreting Pituitary Adenomas by Magnetic Resonance Imaging in Children and Adolescents with Cushing Disease

Dalia Batista,* Nickolas A. Courkoutsakis,* Edward H. Oldfield, Kurt J. Griffin, Meg Keil, Nickolas J. Patronas, and Constantine A. Stratakis

*Department of Diagnostic Radiology (N.A.C., N.J.P.), Warren Grant Magnuson Clinical Center, National Institutes of Health, Bethesda, Maryland 20892; Section on Endocrinology and Genetics (D.B., N.A.C., K.J.G., M.K., C.A.S.), Developmental Endocrinology Branch, National Institute of Child Health and Human Development, Bethesda, Maryland 20892; Surgical Neurology Branch (E.H.O.), National Institute of Neurological Diseases and Stroke, Bethesda, Maryland 20892*

**Context:** We recently showed that pre- and postcontrast spoiled gradient-recalled acquisition in the steady-state (SPGR) was superior to conventional pre- and postcontrast T-1 weighted spin echo (SE) acquisition magnetic resonance imaging (MRI) for the diagnostic evaluation of pituitary tumors in adult patients.

**Objective:** The present investigation assessed the use of SPGR *vs.* SE-MRI in the diagnostic evaluation of ACTH-secreting tumors in children and adolescents with Cushing disease.

**Design:** Data were analyzed retrospectively from a series of patients seen over 7 yr (1997–2004).

**Setting:** The setting for this study was a tertiary care referral center.

**Patients:** Thirty children with Cushing disease (13 females and 17 males with a mean age of 12 ± 3 yr) were studied.

**Interventions and Outcome Measures:** Imaging results were compared with surgical and pathological findings and the clinical outcome.

**Results:** Twenty-eight patients had microadenomas, and two had macroadenomas; the latter were identified by both MRI techniques. Precontrast SE and SPGR-MRI identified four and six of the microadenomas, respectively. Postcontrast SPGR-MRI identified the location of the tumor in 18 of 28 patients, whereas postcontrast SE-MRI identified the location and accurately estimated the size of the tumor in only five patients ($P < 0.001$).

**Conclusions:** We conclude that conventional MRI, even with contrast enhancement, mostly failed to identify ACTH-secreting microadenomas in children and adolescents with Cushing disease. Postcontrast SPGR-MRI was superior to SE-MRI and should be used in addition to conventional SE-MRI in the pituitary evaluation of children and adolescents with suspected Cushing disease. **(*J Clin Endocrinol Metab* 90: 5134–5140, 2005)**

DETECTION OF ADENOMAS in the pituitary gland by imaging techniques has always been problematic. ACTH-secreting adenomas, in particular, have been proven difficult to localize because these tumors are typically very small (1–7). Magnetic resonance imaging (MRI) has been considered for the last 2 decades as the imaging method of choice for detection of these tumors (1–8). Various modifications of MRI techniques have been proposed to improve the rate of tumor detection (7, 9–12). However, and although MRI sensitivity for pituitary microadenomas varies widely among different investigators, it is generally accepted that these tumors are correctly identified by MRI only in approximately half of the cases (1, 2, 4–7, 10–12). One of the main reasons for misdiagnosis is that pituitary tumors and the surrounding normal pituitary gland often exhibit similar signal and enhancing characteristics (2, 7, 11–15).

Successful treatment of ACTH-secreting adenomas requires accurate diagnosis and exact localization. Because of limitations of imaging (12), many institutions use petrosal sinus sampling (PSS) to distinguish a pituitary from an ectopic source of ACTH. Although PSS has high diagnostic accuracy, it is an invasive and expensive test that is not widely available and carries a finite risk of serious complications. It is also difficult to perform in young children, who have the added risks of sedation or anesthesia. Thus, an improved imaging technique for pituitary tumors in children with Cushing disease would be a significant diagnostic advancement in the work up of these patients.

In a recent pilot study of mostly adult patients, we demonstrated that spoiled gradient-recalled acquisition in the steady-state (SPGR) MRI was superior to the conventional T-1 weighted spin echo (SE) technique in identifying pituitary tumors (11). Because SPGR-MRI can be performed in thin sections of 1 mm thickness, the spatial resolution of the acquired images is substantially improved (16, 17). We hypothesized that this technique might increase the accuracy of

**First Published Online June 7, 2005**

* D.B. and N.A.C. have contributed equally to this work and are thus sharing first authorship.

Abbreviations: $CI_{95}$, 95% Confidence interval; MRI, magnetic resonance imaging; PSS, petrosal sinus sampling; SE, spin echo; SPGR, spoiled gradient-recalled acquisition in the steady-state; TSS, transsphenoidal surgery.

**JCEM is published monthly by The Endocrine Society (http://www.endo-society.org), the foremost professional society serving the endocrine community.**

MRI for the detection of ACTH-secreting pituitary adenomas and assist in decreasing morbidity associated with transsphenoidal surgery (TSS) for Cushing disease in childhood (18–21). To evaluate this possibility, we compared the results of MRI using the SPGR technique and the conventional T1-weighted SE technique in 30 children with Cushing disease and surgically proven ACTH-secreting microadenomas.

## Patients and Methods

### *Patients and protocol*

A total of 30 patients (Table 1) were studied that were admitted consecutively to the National Institutes of Health-Warren Magnuson Clinical Center from January 1997 to August 2003, under investigational protocol 97-CH-0076, after an institutional review board approval and individual patient consents. The mean age was 12 ± 3 yr (mean and SD), and the group consisted of 13 females and 17 males. Cushing syndrome was diagnosed in all patients by standard testing as described elsewhere (22). After confirmation of hypercortisolism, biochemical testing for Cushing disease included PSS, if the standard T1-weighted SE MRI technique was negative. Twenty-four of our patients underwent PSS for confirmation of Cushing disease, using the procedure that we have described elsewhere (23). All patients underwent TSS for identification and excision of a pituitary adenoma. The size and the exact location of the adenoma were identified at surgery using ring curettes of known diameter. Histopathological examination of the surgical specimen and postoperative biochemical evidence of remission of disease (hypocortisolism) confirmed the diagnosis of an ACTH-secreting adenoma.

### *MRI studies*

All MRI scans were performed in a 1.5 T scanner (Signa, General Electric, Milwaukee, WI). Two imaging techniques were used, coronal precontrast T1-weighted SE with repetition time/echo time of 400/9 msec, 192 × 256 matrix, two excitations, 12-cm field of view, and 3-mm-thick interleaved sections without gap; and coronal precontrast SPGR with repetition time/echo time of 9.6/2.3 msec, a 20° flip angle, 160 × 256 matrix, six excitations, and 12-cm field of view. Contiguous 1.5-mm-thick sections were obtained in all patients. The scan time was approximately 3.4 min. Both SE and SPGR studies were repeated after intravenous administration of 0.01 mmol/kg gadopentetate dimeglumine (Magnevist, Berlex Laboratories, Inc., Mintville, NJ).

### *Data analysis*

For the purposes of the present study, all imaging studies were reviewed retrospectively by two radiologists (N.J.P. and N.A.C.) in a blinded fashion, *e.g.* without knowledge of the surgical outcome and final histology. The radiological interpretation of all images was made first independently by each radiologist; a meeting with the protocol team was then arranged if there was disagreement. A scan was considered positive only if both radiologists agreed either after their first interpretation or their reevaluation after their meeting. Imaging findings were then recorded [presence, size, and position (right, left, central) of any lesion] by the protocol team in a blinded manner. All analyses and comparisons to surgical and histopathologic findings were done by members of the study team that had not participated in the radiological interpretation meetings.

Sensitivity and specificity of both techniques were calculated by comparing the imaging data with the surgical findings, considering the

**TABLE 1.** Imaging findings age, sex, and findings at surgery and histology

| Patient | Age (yr)/sex | SE | SE and contrast | SPGR | SPGR and contrast | Location on imaging | Location at surgery | Size at surgery (mm) |
|---|---|---|---|---|---|---|---|---|
| 1 | 11 M | n.ob. | iso. | n.ob. | hypo-enh. | R | R | 6 |
| 2 | 10 F | n.ob. | iso. | n.ob. | hypo-enh. | L | L | 5.5 |
| 3 | 12 M | n.ob. | iso. | n.ob. | hypo-enh. | L | L | 8 |
| 4 | 8 M | n.ob. | iso. | n.ob. | hypo-enh. | Mid.-L | L | 8 |
| 5 | 14 M | n.ob. | iso. | n.ob. | hypo-enh. | R | R | 4.5 |
| 6 | 8 M | n.ob. | iso. | n.ob. | iso. | non-diagn. | Midline | 3 |
| 7 | 15 F | n.ob. | hypo-enh. | n.ob. | iso. | non-diagn. | L | 5 |
| 8 | 12 M | hypo-int. | iso. | hypo-int. | hypo-enh. | L | L | 7 |
| 9 | 12 M | hypo-int. | iso. | hypo-int. | hypo-enh. | R | R | 8 |
| 10 | 11 M | n.ob. | iso. | n.ob. | hypo-enh. | Midline | Midline | 3.5 |
| 11 | 16 F | n.ob. | hypo-enh. | hypo-int. | hypo-enh. | R | R | 8 |
| 12 | 13 M | n.ob. | iso. | n.ob. | iso. | non-diagn. | Midline | 4 |
| 13 | 13 M | n.ob. | iso. | n.ob. | iso. | non-diagn. | L | 8 |
| 14 | 10 M | n.ob. | iso. | n.ob. | hypo-enh. | L | Mid.-L | 4 |
| 15 | 15 F | hypo-int. | hypo-enh. | hypo-int. | hypo-enh. | R | R | macroad. |
| 16 | 11 F | n.ob. | hypo-enh. | n.ob. | hypo-enh. | L | L | 6 |
| 17 | 17 F | n.ob. | iso. | n.ob. | hypo-enh. | R | R | 3.5 |
| 18 | 13 F | n.ob. | hypo-enh. | hypo-int. | hypo-enh. | R | Mid.-R | 8 |
| 19 | 14 F | n.ob. | iso. | n.ob. | iso. | non-diagn. | R | 4.5 |
| 20 | 14 M | hypo-int. | iso. | hypo-int. | hypo-enh. | Midline | Midline | 2.5 |
| 21 | 8 M | n.ob. | iso. | n.ob. | iso. | non-diagn. | Midline | 3 |
| 22 | 16 F | hypo-int. | hypo-enh. | hypo-int. | hypo-enh. | R | R | macroad. |
| 23 | 12 F | n.ob. | iso. | n.ob. | hypo-enh. | R | Midline | 3 |
| 24 | 7 M | n.ob. | iso. | n.ob. | hypo-enh. | L | Midline | 10 |
| 25 | 12 F | Not-av. | not-av. | n.ob. | iso. | non-diagn. | Midline | 9 |
| 26 | 14 F | n.ob. | iso. | n.ob. | iso. | non-diagn. | R | 3 |
| 27 | 6 F | n.ob. | iso. | n.ob. | iso. | non-diagn. | Midline | 4 |
| 28 | 13 M | n.ob. | iso. | n.ob. | hypo-enh. | R | R | 4 |
| 29 | 13 M | n.ob. | iso. | n.ob. | iso. | non-diagn. | R | 6.5 |
| 30 | 12 M | n.ob. | hypo-enh. | not-av. | hypo-enh. | R | R | 5 |

n.ob., Nonobvious lesion; hypo-int., lesion with lower signal compared to the rest of the pituitary gland tissues (in precontrast studies); hypo-enh., hypo-enhancing lesion compared to the rest of the pituitary gland tissue (in postcontrast studies); iso., isoenhancing lesion compared to the rest of the pituitary gland tissue (in postcontrast studies); post. lobe, tumor located within the posterior lobe of the pituitary gland; non-diagn., nondiagnostic imaging evaluation; R, tumor located at the right side; L, tumor located at the left side; Mid.-L or Mid.-R, tumor located at the midline to the left or right side of the anterior lobe of the pituitary; not-av., not available; macroad., macroadenoma; M, male; F, female.

surgical results to represent the gold standard (Table 2). The difference between the sensitivities of both imaging techniques were calculated using a sample test of correlated proportion (Table 3); 95 percent confidence intervals ($CI_{95}$) were then calculated (24, 25). Differences in tumor size were compared by paired Student's *t* tests. $P < 0.05$ was considered significant.

## Results

### *Imaging findings*

All tumors detected on the precontrast scans were hypodense; likewise, all lesions identified on the postcontrast scans demonstrated decreased enhancement with respect to the normal pituitary parenchyma regardless of the technique (SE or SPGR) (Fig. 1). When tumors were visible by both techniques, the SPGR technique generally provided a sharper, clearer image (compare Fig. 1, B with C). Two patients had a macroadenoma and were identified by both techniques. Although the largest tumors were identified with both methods, the smaller tumors were only seen with the SPGR technique (Table 1). No tumors found on the SE-MRI were missed by the SPGR scans. No patients with a microadenoma missed on the postcontrast scans had an indirect sign of a pituitary tumor (such as deviation of the stalk or unilateral superior convexity) that could have assisted in the correct diagnosis (2, 9). There was no good correlation between PSS and imaging findings. PSS was performed in 24 of the 30 children; localization of the tumor by PSS was correct in approximately only 50% of the cases, but a larger investigation of PSS data in children is currently ongoing (Batista, D., and C. A. Stratakis, unpublished data).

### *Surgical findings and outcome*

No children with ectopic ACTH production were identified. All 30 patients (Table 1) were in remission immediately after TSS, confirmed by undetectable levels of urinary free cortisol postoperatively; however, recently we identified two patients that recurred and in whom histology had identified ACTH-producing cells. These two patients, who also had a negative MRI, were considered as having negative surgical exploration (Table 2), although the surgical report identified a lesion in each case (Table 1). For one of these patients, precontrast SE- and SPGR-MRI studies were not available; in an additional two patients with negative MRIs, the tumor was not found in the first exploration (listed as a negative surgical result in Table 2), but eventually a tumor was found in a second procedure, and its size and location are recorded in Table 1.

In two adolescent patients, a macroadenoma was evident by both SE and SPGR techniques. TSS identified adenomas with vertical diameters measuring 22 and 18 mm, respectively. The remaining patients had microadenomas (size < 1 cm), with nine found on the right, eight on the left side, and 11 near the midline of the gland. Histologic examination did not reveal tissue degeneration, cyst formation, hemorrhage, or necrosis in any of the excised adenomas. The size of the microadenomas varied from 2.5–10 mm; there were no significant differences between the mean size of the tumor at the time of surgery *vs.* that in postcontrast SPGR-MRI (7.6 ± 0.4 *vs.* 5.6 ± 0.98, respectively; $P = 0.15$).

**TABLE 2.** Localization of a microadenoma by imaging method and at surgery

| | Surgery | |
|---|---|---|
| | + | − |
| Precontrast SE-MRI | | |
| + | 4 | 1[a] |
| − | 21 | 2[b] |
| Postcontrast SE-MRI | | |
| + | 5 | 2[b] |
| − | 19 | 2[b] |
| Precontrast SPGR-MRI | | |
| + | 6 | 1[a] |
| − | 19 | 2[b] |
| Postcontrast SPGR-MRI | | |
| + | 18 | 2[b] |
| − | 6 | 2[b] |

Plus sign (+) identifies the presence of an adenoma in the pituitary by respective imaging study (column) and at surgery (row).

[a] Precontrast SE and SPGR MRIs were not available for patients 25 and 30; SE-MRI with contrast was not available in patient 25 (see Table 1).

[b] Two patients did not have an adenoma identified during their first surgery; a second procedure, shortly after the first one, identified an ACTH-producing lesion (their size and location are listed in Table 1). For an additional two patients, a tumor was recorded in surgery and immunostaining confirmed its ACTH production; however, these patients recently recurred and were also included as "negative" for surgical localization in this table.

**TABLE 3.** Overall comparison between postcontrast SE-MRI and SPGR-MRI-detection of a pituitary corticotropinoma

| | Postcontrast SPGR-MRI | | Total[a] |
|---|---|---|---|
| | + | − | |
| Postcontrast SE-MRI | | | |
| + | 5 | 0 | 5 |
| − | 13 | 8 | 21 |

[a] For this analysis, only 26 cases (of the total 30) were included; two tumors were excluded because they were macroadenomas; two children were not cured (see text).

### *Data analysis: SE- vs. SPGR-MRI*

Two patients had a macroadenoma and were identified by both techniques; these patients were excluded from this analysis. When we compared imaging results *vs.* surgical findings in the remaining patients (Table 2), in the precontrast SE-MRI, 14.2% (four of 28) patients had a microadenoma. In the postcontrast SE-MRI, 18% (five of 28) of the patients had a microadenoma that was identified correctly after taking into account the surgical report. In contrast, in SPGR-MRI, in the precontrast study, 21% (six of 28) of the patients had a microadenoma; after contrast enhancement, SPGR-MRI identified an adenoma in 64% (18 of 28) of the patients.

When the sensitivity was calculated comparing imaging testing *vs.* the location of the adenoma at surgery (Table 2), the sensitivity for SE-MRI (precontrast T1) was 16% (four of 25; $CI_{95}$, 5- 40%), and the specificity was 66.7% (two of three; $CI_{95}$, 13–98%). For the postcontrast SE-MRI, the estimated sensitivity was better at 21% (five of 24; $CI_{95}$, 8–43%), with a specificity of 50% (two of four; $CI_{95}$, 9–90%). However, the corresponding values for SPGR-MRI were significantly higher. The sensitivity for precontrast SPGR-MRI was 24% (six of 25; $CI_{95}$, 8–41%), and specificity was 67% (two of three;

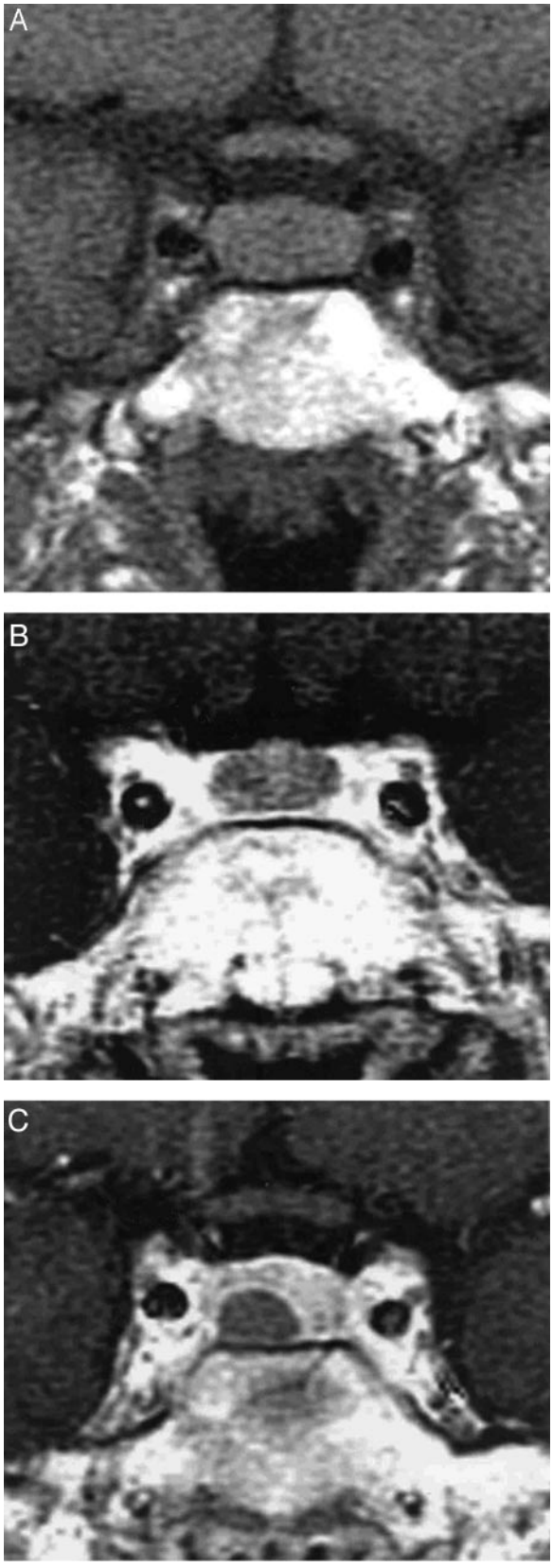


FIG. 1. MRI studies of a patient with a corticotropinoma detected by both SE- and SPGR-MRI in postcontrast studies. This is one of the largest microadenomas encountered in this series. A, Coronal precontrast SE images revealed no abnormality. B, Coronal postcontrast SE images demonstrated a homogeneously hypoenhancing area in the right side of the anterior pituitary lobe. C, Coronal postcontrast SPGR images identified an adenoma in approximately the same location as the enhanced SE scan. Although the adenoma was identified by both studies, the contrast between normal and abnormal tissues is superior on the SPGR images. The tumor location was confirmed at surgery.

$CI_{95}$, 13–98%). For the postcontrast SPGR MRI, sensitivity was 75% (18 of 24; $CI_{95}$, 53–89%), and the specificity was 50% ($CI_{95}$, 9–91%). The difference between the sensitivities of the postcontrast SE-MRI *vs.* that of the SPGR-MRI was quite significant at 55% ($CI_{95}$, 36–74%; $P = 0.001$) (Table 3).

Both techniques had high false-negative rates, but the numbers for SPGR-MRI were significantly better. For SE-MRI (postcontrast), this was 90% ($CI_{95}$, 68–98%) with a false-positive rate of 28% ($CI_{95}$, 5–70%). For SPGR-MRI (postcontrast), the values were 75% ($CI_{95}$, 36–96%) and 10% ($CI_{95}$, 2–33%), respectively. Finally, the overall probability that postcontrast SE-MRI would be positive in a child with surgically proven Cushing disease was 25% ($CI_{95}$, 11–45%), whereas the probability that it would be negative was 75% ($CI_{95}$, 55–86%). On the other hand, for postcontrast SPGR-MRI, the probability that the test would be positive was 71% ($C_{95}$, 51–86%), whereas the probability that the test would be negative was 29% ($CI_{95}$, 14–50%). Two representative examples of patients with negative SE-MRIs but positive SPGR-MRIs are shown in Figs. 2 and 3; in the latter, the use of contrast enhancement identified a lesion that was not visible by plain SPGR-MRI, too.

## Discussion

Our overall success rate for TSS for Cushing disease at the National Institutes of Health for the period 1997–2004 is 97.6% (without long-term follow up data; Stratakis, C. A., and E. H. Oldfield, unpublished data). The SPGR technique improved by approximately 2-fold the detection rate by MRI of pituitary adenomas in a pilot study of mostly adult patients (11). In adults, SE-MRI (postcontrast) had a detection rate of 49% ($CI_{95}$, 34–63%), whereas that of the SPGR-MRI (postcontrast) was 80% ($CI_{95}$, 68–91%) (11).

Cushing disease is extraordinarily rare in children and adolescents (19–21). The majority of pediatric patients with Cushing disease have small microadenomas as the cause of their disease; in addition, pituitary incidentalomas are rare in children (20–22, 26). The present study is the largest that specifically evaluated the use of any type of MRI for detection of pituitary corticotropinomas in children, but we also evaluated a new modality, SPGR-MRI. The detection rate of 64% with a sensitivity of 75% represents a significant improvement over conventional imaging techniques that are currently in use.

The low detection rate of these tumors in children by conventional imaging, which in the present study was at approximately 20%, was less than half of that reported in adults (1, 7, 11). Possible explanations for this difference are the relatively smaller size of ACTH-secreting adenomas in children (22) and the absence of tissue degeneration, necrosis, or cyst formation in pituitary adenomas of younger patients (24). These tissue changes provide additional elements

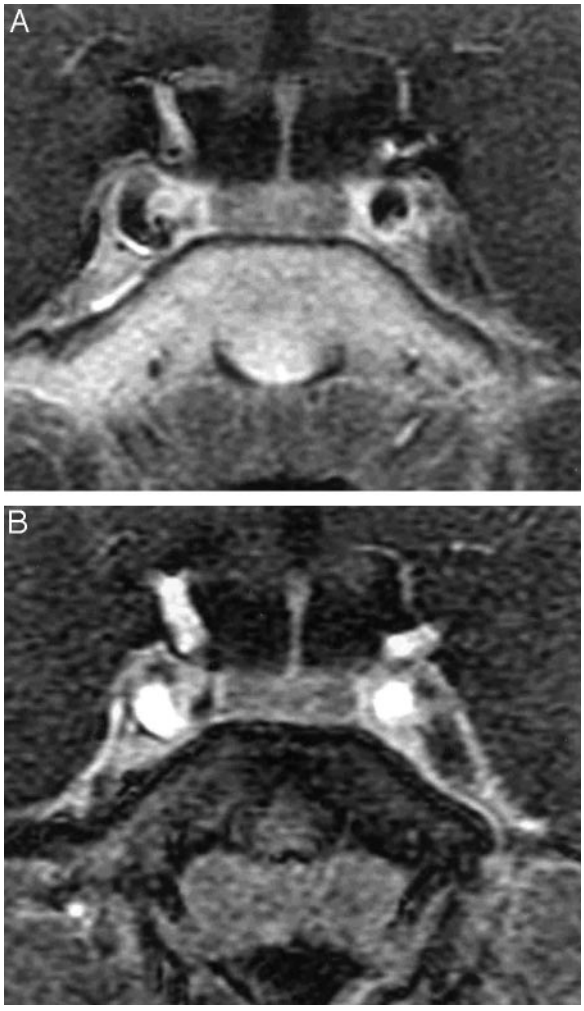


FIG. 2. MRI studies of a patient with a corticotropinoma detected only by SPGR-MRI (postcontrast). A, Coronal postcontrast SE-MRI. There is no evidence of adenoma in the pituitary gland. B, Coronal postcontrast SPGR-MRI demonstrates an adenoma, an area of slightly diminished enhancement is identified on the left half of the pituitary. The tumor location was confirmed at surgery.

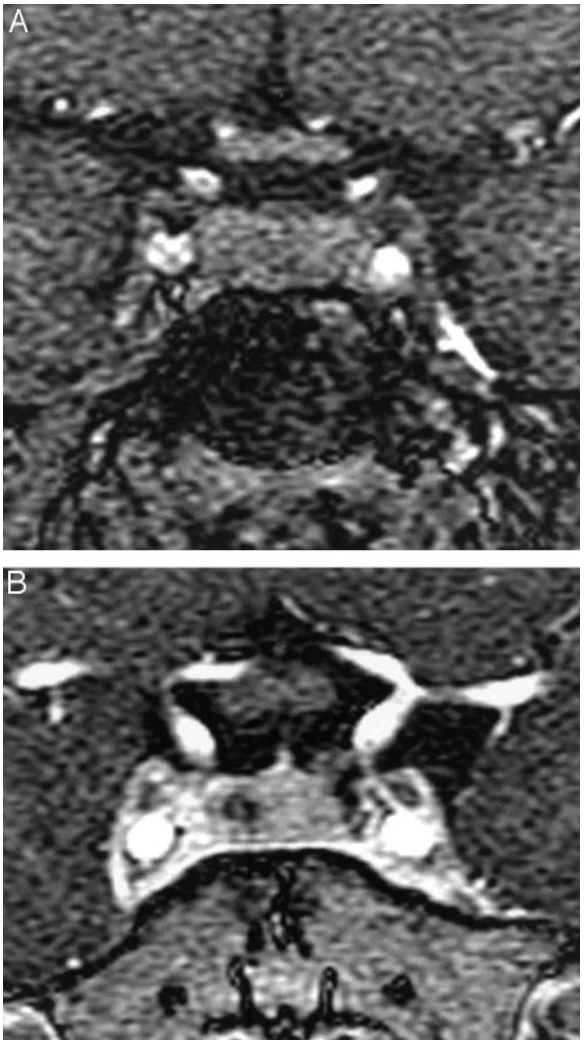


FIG. 3. MRI studies of a patient with a corticotropinoma detected only by SPGR-MRI (postcontrast). A, Coronal precontrast SPGR-MRI. The pituitary enhanced homogeneously, and there was no evidence of an adenoma in the anterior lobe of the gland. B, Coronal postcontrast SPGR-MRI showed an adenoma, as an inhomogeneously hypoenhancing area on the right side of the adenohypophysis. The tumor location was confirmed at surgery.

of separation from adjacent normal tissue, which make the presence of an adenoma more obvious upon radiological studies (2, 5, 6).

A number of factors may account for the apparent superior performance of the SPGR compared with the SE technique (7–12). The increased soft tissue contrast with SPGR is well-acknowledged; with it, images can be obtained with 1.5-mm-thin sections (16, 17) (Fig. 1). SE imaging, on the other hand, is usually obtained with 3-mm thickness, and averaging of different tissues can obscure smaller pituitary microadenomas (7–11). The main drawback of the SPGR technique is its inferior signal to noise ratio compared with SE-MRI (11, 16, 17). In this study, we doubled the number of excitations from three to six to alleviate this problem. In doing so, the specificity of the findings was improved, whereas the scan time was still shorter than that of the SE technique, thus, minimizing motion artifacts that can be encountered with prolonged scanning.

As was the case in adult patients (11), we were surprised to detect pituitary tumors in pediatric patients who were referred after a previously negative MRI had been obtained elsewhere. Is it possible that these tumors grew sufficiently in the interval between the two studies to allow detection? Although this is a possibility, it is unlikely because our imaging usually took place within 6 months from the previous study. First, pituitary tumors typically do not increase in size over an interval of only a few months. Second, the tumors that were detected by SPGR-MRI in the course of our study, after a recent negative MRI elsewhere, covered the same range of sizes as other corticotropinomas that have been reported in the literature (1, 2, 11); a recent size increase would suggest that the newly detectable tumors would be, on average, of smaller size. Third, in the previous study (11), we reviewed films obtained at other institutions and found

a great variability in the technical aspects of the scanning procedure and, consequently, the quality of imaging (11). Optimal detection of pituitary adenomas requires the use of imaging techniques developed for pituitary studies, not brain; it is generally better if these studies, especially in children, are obtained at specialized, tertiary referral centers for Cushing disease (26).

The difference in the rate of detection using the two techniques was not statistically different in the pediatric population, whereas in adult patients, there were too few patients with false-positive findings to make a meaningful comparison (11). The false-positive rate in pediatric patients was 28% ($CI_{95}$, 5–70%) and 10% ($CI_{95}$, 2–33%) for the SE- and SPGR-MRI (postcontrast), respectively. This is comparable with the 18–20% rates reported by other centers for conventional pituitary MRI but contrasts with the 4% rate found in the study of adult patients (11) and the 0% rates in earlier studies from the National Institutes of Health (1). It is possible, therefore, that SPGR-MRI, at least in children, increases the chances of falsely detecting a pituitary tumor. From the surgical and pathological findings, we know that MRI-detected abnormalities did not represent additional pituitary lesions, which in some cases of Cushing disease may coexist (27).

The surgical cure rate for Cushing disease is 80–90% when MRI localizes a tumor but drops to 50–70% when the lesion cannot be demonstrated upon preoperative imaging (28–31). Because in a patient with endocrine testing consistent with Cushing disease a positive MRI almost always indicates the site of the ACTH-secreting adenoma, as it did in the current series, and because pituitary exploration with multiple incisions in the gland can produce hypopituitarism in some patients, our surgeon (E.H.O.) begins exploration for the adenoma based on the site of the positive MRI. If a tumor is found there, the tumor is removed, and no further exploration of the gland is performed. Thus, the correct localization of the tumor on MRI not only provides higher remission rates, but also, by limiting the exploration of the pituitary gland that is necessary, it may reduce the incidence of postoperative complications, such as cerebrospinal fluid leak and hypopituitarism. Suggestive localization on MRI guides the surgeon during TSS, even if the imaging study was not definitive (32).

We conclude that coronal postcontrast SPGR images should be added to conventional SE imaging protocols of the pituitary gland. SE images are complementary to SPGR images for the diagnosis of corticotropinomas, and both techniques should be used for the investigation of the pituitary gland in all patients with Cushing syndrome. Although imaging alone cannot establish the diagnosis of Cushing disease in patients with Cushing syndrome, it plays a crucial supporting role to diagnostic endocrine testing.

## Acknowledgments

We thank, first, our patients who participated in National Institute of Child Health and Human Development 97-CH0076 investigational protocol (Principal Investigator, C.A.S.) and, second, Dr. Alicia Y. Toledano (Center for Statistical Sciences at Brown University, Providence, RI) for her review of our statistical analysis and presentation.

Received September 7, 2004. Accepted May 31, 2005.

Address all correspondence and requests for reprints to: Dr. Constantine A. Stratakis, Section on Endocrinology and Genetics, Developmental Endocrinology Branch, National Institute of Child Health and Human Development, National Institutes of Health, Building 10, Room 10N262, 10 Center Drive, MSC 1862, Bethesda, Maryland 20892-1862. E-mail: stratakc@mail.nih.gov.

Present address for N.A.C.: Department of Radiology, Medical School, Democritos University of Thrace, 68100 Alexandroupolis, Greece.

## References

1. **Dwyer AJ, Frank JA, Doppman JL, Oldfield EH, Hickey AM, Cutler GB, Loriaux DL, Schiable TF** 1987 Pituitary adenomas in patients with Cushing disease: initial experience with Gd-DTPA-enhanced MR imaging. Radiology 163:421–426
2. **Doppman JL, Frank JA, Dwyer AJ, Oldfield EH, Miller DL, Nieman LK, Chrousos GP, Cutler GB, Loriaux DL** 1988 Gadolinium DTPA enhanced MR imaging of ACTH-secreting microadenomas of the pituitary gland. J Comp Assist Tomogr 12:728–735
3. **McPherson P, Hadley DM, Teasdale E, Teasdale G** 1989 Pituitary microadenomas. Does gadolinium enhance their demonstration? Neuroradiology 31: 293–298
4. **Sakamoto Y, Takahashi M, Korogi Y, Bussaka H, Ushio Y** 1991 Normal and abnormal pituitary glands: gadopentetate dimeglumine-enhanced MR imaging. Radiology 178:441–445
5. **Nakamura T, Schorner W, Bittner RCh, Felix R** 1988 The value of paramagnetic contrast agent gadolinium-DTPA in the diagnosis of pituitary adenomas. Neuroradiology 30:481–486
6. **Kucharczyk W, Davis DO, Kelly WM, Sze G, Norman D, Newton TH** 1986 Pituitary adenomas: high resolution MR imaging at 1.5 T. Radiology 161:761–765
7. **Peck WW, Dillon WP, Norman D, Newton TH, Wilson CB** 1989 High-resolution MR imaging of pituitary microadenomas at 1.5 T: Experience with Cushing Disease. Am J Radiol 152:145–151
8. **Kucharczyk W, Bishop JE, Plewers DB, Keller MA, George S** 1994 Detection of pituitary microadenomas: comparison of dynamic keyhole fast spin-echo, unenhanced and conventional-spin echo, unenhanced and conventional contrast-enhanced MR imaging. Am J Roentgenol 163:671–679
9. **Miki Y, Matsuo M, Nishizawa S, Kuroda Y, Keyaki A, Makita Y, Kawamura J** 1990 Pituitary adenomas and normal pituitary tissue: enhancement patterns on gadopentetate-enhanced MR imaging. Radiology 177:35–38
10. **Bartynski WS, Lin L** 1997 Dynamic and conventional spin-echo MR of pituitary microlesions. Am J Neuroradiol 18:965–972
11. **Patronas NJ, Bulakbasi N, Stratakis CA, Lafferty A, Oldfield EH, Doppman J, Nieman LK** 2003 Spoiled gradient recalled acquisition in the steady state technique is superior to conventional postcontrast spin echo technique for magnetic resonance imaging detection of adrenocorticotropin-secreting pituitary tumors. J Clin Endocrinol Metabol 88:1565–1569
12. **Davis WL, Lee JN, King BD, Harnsberger HR** 1994 Dynamic contrast enhanced MR imaging of the pituitary gland with fast spin-echo technique. J Magn Reson Imag 4:509–511
13. **Richmond IL, Wilson CB** 1978 Pituitary adenomas in childhood and adolescence. J Neurosurg 49:163–168
14. **Haddad SF, VanGilder JC, Menezes AH** 1991 Pediatric pituitary tumors. Neurosurgery 4:509–514
15. **Partington MD, Dudley HD, Laws ER, Schitauer BW** 1994 Pituitary adenomas in childhood and adolescence. J Neurosurg 80:209–216
16. **Yoshioka H, Alley M, Steines D, Stevens K, Rubesova E, Genovese M, Dilingham MF, Lang P** 2003 Imaging of articular cartilage in osteoarthritis of the knee joint: 3D spatial-head spoiled gradient echo vs. fat-suppressed 3D spoiled gradient-echo MR imaging. J Magn Reson Imaging 18:66–71
17. **Naganawa S, Koshikawa T, Fukatsu H, Ishigaki T, Nakashima T, Ichinose N** 2002 Contrast-enhanced MR imaging of the endolymphatic sac in patients with sudden hearing loss. Eur Radiol 12:1121–1126
18. **Etxabe J, Vazquez JA** 1994 Morbidity and mortality in Cushing's disease: an epidemiological approach. Clin Endocrinol (Oxf) 40:479–484
19. **Mindermann T, Wilson CB** 1994 Age-related and gender-related occurrence of pituitary adenomas. Clin Endocrinol (Oxf) 41:359–364
20. **Artese R, D'Osvaldo DH, Molocznik I, Benencia H, Oviedo J, Burman JA, Basso A** 1998 Pituitary tumors in adolescent patients. Neurol Res 20:415–417
21. **Ludecke DK, Flitsch J, Knappe UJ, Saeger W** 2001 Cushing's disease: a surgical view. J Neurooncology 54:151–166
22. **Magiakou MA, Mastorakos G, Oldfield EH, Gomez MT, Doppman JL, Cutler Jr GB, Nieman LK, Chrousos GP** 1994 Cushing's syndrome in children and adolescents. Presentation, diagnosis, and therapy. N Engl J Med 331:629–636

23. **Oldfield EH, Doppman JL, Nieman LK, Chrousos GP, Miller DL, Katz DA, Cutler Jr GB, Loriaux DL** 1991 Petrosal sinus sampling with and without corticotropin-releasing hormone for the differential diagnosis of Cushing's syndrome. N Engl J Med 325:897–905
24. **Hawass NE** 1997 Comparing the sensitivities and specificities of two diagnostic procedures performed on the same group of patients. Br J Radiol 70: 360–366
25. **Levin JR, Serlin RC** 2000 Changing students' Perspectives of McNemar's Test of Change. J Stat Educ 8:1–11
26. **Daughaday WH** 1984 Cushing's disease and basophilic microadenomas. N Engl J Med 310:919–920
27. **Hall WA, Luciano MG, Doppman JL, Patronas NJ, Oldfield EH** 1994 Pituitary magnetic resonance imaging in normal human volunteers: occult adenomas in the general population. Ann Intern Med 120:817–820
28. **Moshang Jr T** 2003 Cushing's disease, 70 years later. And the beat goes on. J Clin Endocrinol Metab 88:31–33
29. **Ratliff JK, Oldfield EH** 2000 Multiple pituitary adenomas in Cushing's disease. J Neurosurg 93:753–761
30. **Barrou Z, Abecassis JP, Guilhaume B, Thomopoulos P, Bertagna X, Derome P, Bonnin A, Luton JP** 1997 Magnetic resonance imaging in Cushing disease. Prediction of surgical results. Presse Med 26:7–11
31. **Bochicchio D, Losa M, Buchfelder M** 1995 Factors influencing the immediate and late outcome of Cushing's disease treated by transsphenoidal surgery: a retrospective study by the European Cushing's Disease Survey Group. J Clin Endocrinol Metab 80:3114–3120
32. **Buchfelder M, Nistor R, Fahlbusch R, Huk WJ** 1993 The accuracy of CT and MR evaluation of the sella turcica for detection of adrenocorticotrophic hormone-secreting adenomas in Cushing disease. Am J Neuroradiol 14:1183–1190

**JCEM is published monthly by The Endocrine Society (http://www.endo-society.org), the foremost professional society serving the endocrine community.**